Int J Clin Exp Med 2023;16(8):166-178
www.ijcem.com /ISSN:1940-5901/IJCEM0136995

Original Article

Chitosan/siRNA nanoparticles targeting connective tissue growth factors reduce scar hyperplasia in a rabbit ear model

Haibin Wu[1*], Linling Cheng[2*], Jing Qin[1], Yongjun Zheng[3]

[1]Department of General Surgery, General Hospital of Central Theater Command, The People's Liberation Army, Wuhan 430070, Hubei, China; [2]University of Colorado Anschutz Medical Campus, Denver, CO, USA; [3]Burns Center of Changhai Hospital, The Second Military Medical University, Shanghai 200433, China. [*]Co-first authors.

Received July 4, 2021; Accepted May 23, 2023; Epub August 15, 2023; Published August 30, 2023

Abstract: Hypertrophic scars are closely related to the sustained activation of transforming growth factor β (TGF-β)/Smads signaling pathway. As a terminal molecule of this signaling pathway, connective tissue growth factor (CTGF) can be overexpressed and thus induce fibroblast proliferation and extracellular matrix deposition. This study aimed to examine whether the expression of CTGF can be inhibited by chitosan-siCTGF (Cs-siCTGF) nanoparticles, thereby reducing scars during wound healing. Cs-siCTGF nanoparticles were formed through electrostatic interaction, and the nanoparticle size can be confirmed through Nano ZS Zetasizer and transmission electron microscopy. For obtaining the loading efficiency and controlled release properties, the nanoparticles were applied to fibroblasts, the transfection and uptake efficiency of siCTGF loaded chitosan nanoparticles were examined. At last, we tested the RNA interference in a rabbit model of hypertrophic scar. Results showed that the expression of CTGF was down-regulated, both α-smooth muscle actin (α-SMA) expression and extracellular matrix deposition were reduced. All of these factors contributed to the extenuation of scar after wound healing. This finding suggests that Cs-siCTGF nanoparticles may be as a promising agent for prevention of hypertrophic scars.

Keywords: Hypertrophic scars, connective tissue growth factor (CTGF), chitosan-siCTGF (Cs-siCTGF), nanoparticles

Introduction

Every year, millions of people develop scars caused by skin injury, such as surgery, trauma, or burns, which can remarkably affect the patients' quality of life [1]. In order to prevent and treat hypertrophic scarring, many treatments have emerged, including surgery, silicone gel application, topical corticosteroids, sheet application, and so on. However, treatments for hypertrophic scar are currently widely questioned by clinicians due to invalid outcomes. Besides, the pathogenesis of hypertrophic scar formation remains unclear. The transforming growth factor β (TGF-β)/Smads signaling pathway is essential for fibrosis, which affects the skin and other organs [2-6]. In previous studies, scarring is inhibited by blocking of TGF-β, Smad2, or Smad3 [7, 8]. With the widespread effects of TGF-β or Smads genes, inhibition of their profibrotic effects may weaken their immunomodulatory functions, which are also essential for wound healing [9, 10]. Study found that inhibition of TGF-β can delay wound healing [11]. Therefore, the direct targeting of TGF-β or Smads genes may influence the overall effectiveness.

Connective tissue growth factor (CTGF) is a terminal downstream effector of the TGF-β/Smads signaling pathway and is very important for wound healing. Up-regulation of CTGF expression can promote wound healing. However, there are still controversial results remaining. Some studies have reported wound healing is unaffected when the CTGF expression is inhibited [12]; others have found that down-regulation of CTGF expression can delay wound healing [13, 14]. Besides, CTGF can promote fibroblast proliferation, extracellular matrix synthesis and secretion and myofibroblast transformation [15]. The pathological overexpres-

sion of CTGF has been found in many fibrotic diseases, including hypertrophic scars [15-18]. Scar formation not only can be minimized by inhibiting the expression of CTGF gene in both in vivo and in vitro, but also effectively hampered by targeting CTGF expression without inducing side effects, which is caused by the intervention of conventional genes, such as TGF-β or Smads [17].

With high efficiency and specificity, small interfering RNA (siRNA) has been used as a disease treatment due to the fact that it can down-regulate the expression of target genes [18, 19]. Antisense siRNA methods can be applied to reduce target gene expression. However, siRNA systemic delivery is limited by several disadvantages, such as poor biodistribution, low stability, and inefficient uptake [20, 21]. Therefore, efficient methods should be developed to control siRNA release and improve therapeutic effects. There are various materials available for encapsulating siRNA and forming nanoparticles. For example, chitosan, is a natural cationic material that possesses low cell toxicity and immunogenicity [22, 23]. Chitosan has been developed as a siRNA carrier because it has a protonatable amine groups, so it can interact with the negatively charged siRNA [24, 25]. When genetic materials are encapsulated by chitosan, nanoparticles were formed, chitosan nanoparticles then can adhere to the cell membrane and efficiently avoid degradation by liposomes [26]. Thus, chitosan-siRNA nanoparticles may be developed as a promising non-viral siRNA delivery vehicle for disease treatment.

In this study, a novel treatment was designed to inhibit scar formation by local injection of Cs-siCTGF nanoparticles to knock down the expression of CTGF after the skin was fully damaged. Data showed that Cs-siCTGF nanoparticles could inhibit fibroblast proliferation and collagen expression. The release time of siCTGF from Cs-siCTGF nanoparticles could be sustained up to 72 hours in vitro. In vivo, Cs-siCTGF nanoparticles were further applied to a rabbit model of hypertrophic scar. These nanoparticles significantly reduced the expression of CTGF and other pro-fibrosis genes. Our results indicated that scar formation can be impeded significantly by using Cs-siCTGF nanoparticles.

Materials and methods

Chitosan-siCTGF (Cs-siCTGF) nanoparticles preparation

Cs-siCTGF nanoparticles were prepared as reported in a previous article [27]. Chitosan (Sigma-Aldrich, Germany) were dissolved in sodium acetate buffer (300 mM of sodium acetate, pH 5.5) and filtered to obtain 1 mg/ml of chitosan working solution. For generation of Cs-siCTGF nanoparticles at 50 nM, 100 nM and 200 nM, approximately 5 μl of 10 μM, 20 μM, and 40 μM siCTGF stock (Shanghai Biotend Biotechnologies Company, China) was added into 1 ml of sodium tripolyphosphate (TPP) solution (Sigma-Aldrich, Germany) to make a siCTGF-TPP solution respectively, subsequently these siCTGF-TPP solutions were added into 3 ml of chitosan working solution to make the Cs-siCTGF nanoparticles solutions. The resulting solutions (Cs-siCTGF nanoparticles solutions) were stirred at 450 rpm for 15 minutes and then allowed to stand at room temperature for 30 minutes. After centrifugation at 16,000×g and at 4°C for 30 minutes, the supernatant contained unentrapped siCTGF was transferred into an additional tube and used as control, and the pellets of Cs-siCTGF nanoparticles were collected and purified through extensive dialysis by using a Spectra/Por® dialysis membrane (Biotech, USA), and eventually resuspended in PBS for using. All of the devices were treated with diethylpyrocarbonate (DEPC)-treated water.

Characterization of the Cs-siCTGF nanoparticles

Morphology: A drop of Cs-siCTGF nanoparticle suspension was attached to a copper film and allowed to be dried at 25°C after 3 minutes. The morphological characteristics of the Cs-siCTGF nanoparticles were observed through transmission electron microscopy (TEM) (Tecnai G2spirit Biotwin, FEI Company, USA).

Mean particle size and polydispersity index (PDI) analysis: The mean particle size and PDI of Cs-siCTGF nanoparticles were determined in DEPC-treated aqueous solution by using Nano ZS Zetasizer (Malvern, UK) at 25°C through laser Doppler velocimetry and dynamic light scattering. In brief, 100 μl of Cs-siCTGF nanoparticle solution was placed in a culvert. The

particle size and PDI were measured by using a size analyzer. Each sample was measured triplicates.

Loading efficiency assay

After the Cs-siCTGF was made, the control solution (unentrapped siCTGF) was collected as mentioned in above and assayed by UV absorbance (Pharmacia, Sweden) at a density wavelength of 260 nm. The encapsulation percentage was calculated as follow: % loading = (total amount of siCTGF - the amount of unentrapped siCTGF)/total amount of siCTGF.

Controlled release assay

When Cs-siCTGF was made, the nanoparticles were resuspended in 100 ml of PBS solution and incubated at 37°C for 6 hours, followed by centrifugation again and the supernatant was collected. The UV absorbance of the supernatant was measured through UV spectrophotometry (Pharmacia, USA) at a density wavelength of 260 nm. The Cs-siCTGF nanoparticles release rate of each time point (0, 6, 12, 24, 36, 48, and 72 hours) was calculated as follows: release percentage = amount of supernatant siCTGF/total amount of siCTGF in nanoparticles × 100%.

Transfection and uptake rate assay

Cy3 labeled Cs-siCTGF nanoparticles (Cs-siCTGF-Cy3) were prepared to observe whether Cs-siCTGF can be absorbed by fibroblasts. In brief, 1 ml of TPP solution containing 5 μl of Cy3-labeled siCTGF (20 μM) was added into 3 ml of chitosan. After stirring for 15 minutes at room temperature, the nanoparticles labeled with Cy3 suspension was formed. After centrifugation, the nanoparticle pellets were obtained and resuspended with DMEM. Two groups were designed for the uptake rate assay: Cy3-labeled siCTGF (si-CTGF-Cy3) group was used as control group, and Cs-siCTGF-Cy3 group was used as treatment group. After one day of incubation, the medium replaced, and the transfection and uptake rate were observed under a fluorescence microscope (Leica, Germany).

siCTGF sequence assay

Three siCTGF sequences were designed to target different regions of the CTGF gene. BLAST was used to analyze the sequence of these siCTGFs and exclude the off-target effect from them. Fibroblasts were transfected with Lipofectamine 2000 (Life Technologies, USA) in accordance with the manufacturer's instructions. In brief, 0.1 nM of siCTGF and 5 μl of Lipofectamine 2000 were added into 250 μl of Opti-MEM medium (Life Technologies, USA) and stand at 25°C for 5 minutes. Lipofectamine 2000 and either siCTGF or scrambled RNA (siNC) in Opti-MEM media were mixed respectively and stand at 25°C for another 20 minutes to form a siCTGF-Lipofectamine complex. Afterward, 500 μl of siCTGF-Lipofectamine complex was added to the fibroblasts. After 24 hours and 48 hours of incubation, whole RNA and proteins were extracted respectively from the transfected fibroblasts for sequencing.

Human fibroblasts culturing

After informed consent was given from participants, the fibroblasts were isolated from human foreskin and cultured as described previously [28], which was approved by the ethics committee of the Second Military Medical University. The dermis was obtained in accordance with the following procedures. The foreskin was digested in 0.25% dispase (Gibco Company, USA) at 4°C for overnight. Separated dermis was then digested in 1% collagenase solution (Gibco Company, USA) at 37°C for 1 hour and filtered. After centrifugation, the fibroblasts were collected and then cultured in DMEM (Gibco Company, USA) with 10% fetal bovine serum (Gibco Company, USA) in a humidified condition of 95% air and 5% CO_2 for appropriated experiments.

Cell toxicity assay

The suspended fibroblasts were plated into 96-well plates (Corning, NY, USA) at a density of 2×10^3 to 5×10^3/well, and each volume of the well was 200 μl. After cell adherent, the medium was collected aside for further experiment. The cells in DMEM medium containing 10% fetal bovine serum were used as a control group, and three different concentrations of Cs-siNC nanoparticles solution (0.5 mg, 1 mg and 2 mg) were applied as experimental groups. After 24 hours incubation, 20 μl of CCK8 solution (Cell Counting Kit 8, Beyontime, China) was added into each well and incubated at 37°C for 3 hours, followed by transferring of

100 μl of the supernatants to another clean 96-well plate. The optical density (OD) value was measured at wavelength of 260 nm by using a multi-plate reader (BioteK, USA) until Day 7.

Quantitative RT-PCR and western blotting assay

Fibroblasts were seeded at a density of 2×10^5 to 5×10^5/well into a 12-well plate (Corning, NY, USA). After one day, the medium was removed and replaced with a fresh DMEM medium. An equal volume of DMEM (blank), nanoparticles formed with naked control chitosan (Cs-siNC) and with various concentration of siCTGF (50 nM, 100 nM and 200 nM) were added into the 12-well plates. After 48 hours incubation, fibroblasts were collected, the expression levels of CTGF and some fibrosis-related genes were assayed through RT-qPCR and western blotting.

RT-PCR: Total RNA extracted from Fibroblasts by RNAzol reagent (Molecular Research Center, Cincinnati, OH, USA) and the concentration was calculated. Isolated RNAs were reverse transcribed into cDNAs by using a PrimeScript™ RT Master Mix (TaKaRa). Relative mRNA expression levels of CTGF, Collagen I and α-SMA were assayed by using a SYBR Premix ex Taq (Takara Bio, Japan), 7500 Real-Time PCR system (Applied Biosystems, Carlsbad, USA) according to the manufacturer's instructions. GAPDH was used as control and 2_DDCt method was used to analysis relative gene expression.

Western blot: Total protein was extracted by using cell lysis buffer (Beyotime, Shanghai, China) and the protein concentration was determined by using the Pierce™ BCA Protein Assay Kit (ThermoFisher Scientific Inc.). Thirty micrograms of protein in each sample (30 ug/lane) were loaded and separated by 10% SDSPAGE and subsequently transferred to 0.45 mm PVDF membranes (Millipore, Bedford, MA, USA). GAPDH rabbit polyclonal anti-CTGF antibody (Abcam, USA), anti-Collagen I antibody (Abcam, USA), anti-α-SMA (Abcam, USA) were incubated with the membrane at 4°C overnight. Then, the membrane was incubated with HRP conjugated goat anti-rabbit (Abcam, USA) antibodies for 1 hour at room temperature. Protein bands were reacted by an ECL detection kit, and the images were analyzed by using the Image-Pro plus 6.0 software.

Cs-siCTGF nanoparticle accumulation and releasing time assay

Nude mice were used to monitor wound fluorescence imaging. A 1 cm × 1 cm of second-degree injury wound on the back skin was made, control siCTGF-Cy3 and Cs-siCTGF-Cy3 were made and injected intradermally from the edge of the wound respectively. At 1, 6, 24, 48, and 72 hours, the mice were anesthetized with 2.5% isoflurane. Fluorescence position and intensity were detected by using an in vivo imaging system (IVIS®200, Caliper LifeSciences, USA). The radiation efficiency of the wound was measured to describe the radiation/lighting power density.

Animal model generation and fibrosis detection assays

The New Zealand white rabbits were housed under standard conditions and treated in accordance with an experimental protocol approved by the Animal Care and Use Committee of the Second Military Medical University. Six-month old rabbits (3-3.5 kg, n=30) were anesthetized with Sodium pentobarbital (30 mg/kg) in vein. Four 10 mm circular wounds were made on the ventral ears of rabbits by punch [29]. Cs-siCTGF nanoparticles were concentrated to 1 mg/ml prior to dosing. Afterward, 20 μl of nanoparticles loaded with 5 μM, 10 μM or 20 μM of siCTGF was injected into each wound at every three days until day 27. The scar thickness of the rabbit ear was measured by using an ultrasonic detector (ALOKA, Japan) at week 4 and week 8. Scar samples were collected at week 4 and week 8. Fibrosis was detected by immunohistochemistry (IHC) staining, western blotting and collagen deposition. Briefly, for IHC staining, sections were deparaffinized, hydrated, and subjected to proteinase K treatment for antigen retrieval. Endogenous peroxidase was blocked by 3% Hydrogen Peroxide/Methanol. The Slides were blocked with normal goat serum and then incubated with corresponding primary antibodies of against Collagen I (Abcam, USA), α-SMA (Abcam, USA) and CTGF (Abcam, USA) overnight at 4°C, respectively. After washing with PBS, the sections were incubated with HRP-conjugated Goat Anti-rabbit IgG (Abcam, USA) and DAB was used for color development. All counting or analyzing procedures of histological images were conducted separately by two pathologists. Western blot

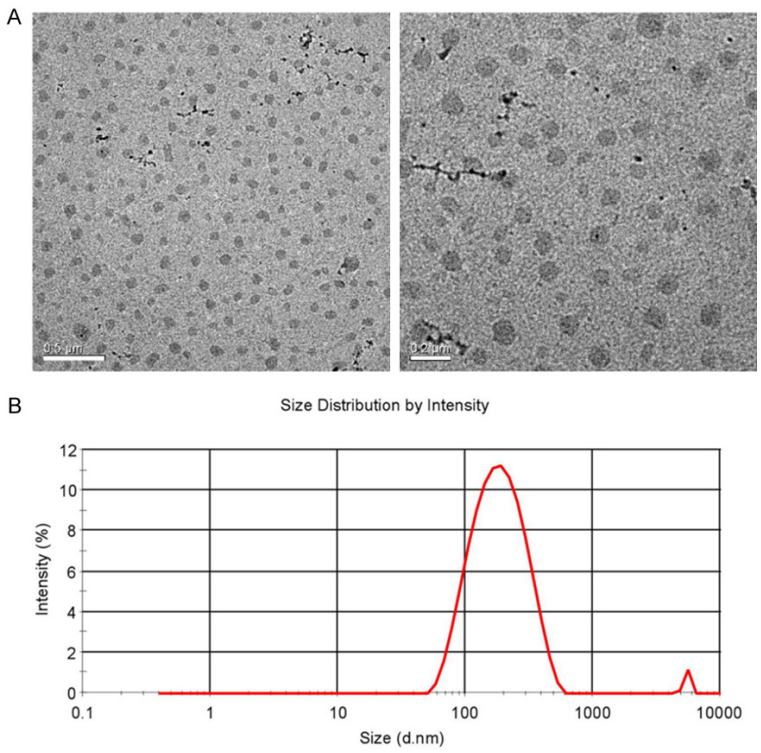

Figure 1. Characterization the formation of Chitosan/siCTGF (Cs-siCTGF) nanoparticles. A. Cs-siCTGF nanoparticles were formed and dropped onto a copper film for detection of morphology. The TEM images showed the Cs-NPs were uniformed in size without adhesion, and the diameters of Cs-siCTGF nanoparticles was 92.6 ± 8.4 nm. B. The mean particle size and polydispersity index (PDI) of Cs-siCTGF nanoparticles were examined by the dynamic light scattering instrument, data revealed a symmetric distribution with an average size of 190.4 ± 3.6 nm.

was carried out as described above with same antibodies. Collagen deposition was observed with Masson's trichrome staining.

Data analysis

Data were statistically analyzed with SPSS16.0 and expressed as mean ± SD. Analysis was conducted with two-tailed Student's t-test. Statistical significance was considered at $P< 0.05$.

Results

Chitosan/siCTGF (Cs-siCTGF) nanoparticles were successfully formed and the roading rate of siCTGF was sufficient

Cs-siCTGF nanoparticles were prepared as it described in the methods. For examining the morphology, the Cs-siCTGF nanoparticles was dropped onto a copper film and transmission electron microscopy (TEM) was applied. The images indicated Cs-siCTGF nanoparticles were uniform in size without adhesion of copper film, and the diameter of it was 92.6 ± 8.4 nm (**Figure 1A**). Further, the mean particle size and polydispersity index (PDI) of Cs-siCTGF nanoparticles were determined by using a dynamic light scattering instrument, and the results revealed Cs-siCTGF nanoparticles were distributed symmetrically and the average of mean particle size was 190.4 ± 3.6 nm (**Figure 1B**). The Polydispersity index (PDI) was 0.233. For determination whether the loading rate of siCTGF was sufficient, the entrapped siCTGF in Cs-siCTGF nanoparticles was formed. The spectrophotometric absorbance of 260 nm was applied, and 97.5% ± 0.5% siCTGF loading rate was achieved.

siCTGF could be sufficiently released from Cs-siCTGF nanoparticles and no toxic to fibroblasts

When Cs-siCTGF was made, the nanoparticles were pelleted and resuspended in PBS, the supernatant was collected for measurement of siCTGF releasing from chitosan nanoparticles. In the first 24 hours, 60% of siCTGF was released, thereafter, 10% of siCTGF was released every 12 hours until 72 hours (**Figure 2B**). For detection the toxicity of Cs-nanoparticles, the fibroblasts were employed. The fibroblasts were isolated from human foreskin and seeded into 96 well plates for assay. Three different concentrations of Cs-siNC nanoparticles (0.5 mg, 1 mg and 2 mg) were made and co-cultured with the cells, then CCK8 kit was applied for evaluation the toxicity of Cs-siCTGF nanoparticles. The OD values were similar in Cs-NP-0.5 mg group and Cs-NP-1 mg group compared with it in the blank group. However, the OD value of the Cs-NP-2 mg group was lower than the other three groups ($P<0.05$) (**Figure 2A**). Therefore, Cs-NP-0.5 mg and Cs-NP-1 mg are best for the further experiments.

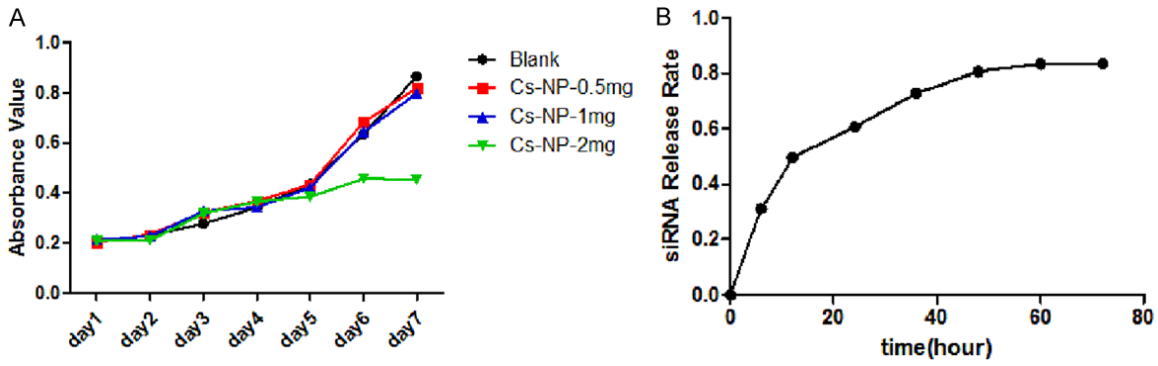

Figure 2. Effect of Cs-siCTGF nanoparticles on fibroblasts. Three different concentrations of Cs-siCTGF nanoparticles (Cs-siCTGF-0.5 mg/ml, Cs-siCTGF-1 mg/ml and Cs-siCTGF-2 mg/ml) were used for co-culture with human fibroblasts. A. Cell toxicity assay. The relative proliferation rate of fibroblasts in the Cs-siCTGF-2 mg group was lower than the other two groups (Cs-siCTGF-0.5 mg and Cs-siCTGF-1 mg) compared with it in control group (Blank) ($P<0.05$). B. siRNA release rate showed, in the first 24 hours, 60% of siCTGF was released. Thereafter, 10% of siCTGF was released every 12 hours until 72 hours.

Cs-siCTGF nanoparticles can be taken up by fibroblasts

To investigate the internalization of Cs-siCTGF nanoparticles, Cy3 dye labeled siCTGF (siCTGF-Cy3) and Cs-siCTGF nanoparticles (Cs-siCTGF-Cy3) were made. The nanoparticles were co-cultured with fibroblasts, and the transfection and uptake rate of nanoparticles were observed under a fluorescence microscope. The cell surface of fibroblasts was stained with Cy3 dye, when the cells took up the siCTGF they appeared as red color. The nucleus was stained with Dapi and appeared as blue color. After the image was merged, the Cy3 (red) appeared around the nuclear dots (blue) in both siCTGF-Cy3 group and Cs-siCTGF-Cy3 group (**Figure 3**). This finding demonstrated that the Cs-siCTGF-Cy3 could be entrapped in fibroblasts.

Selection of the optimal siCTGF sequence

For choose the optimal target regions of the CTGF gene, three siCTGF sequences were designed and transferred into fibroblasts, the silencing efficiency was detected at mRNA and protein levels. The results of quantitative RT-PCR displayed that: there was no significant difference between the blank group and siNC control group, the mRNA level of CTGF was decreased to 85.12% ± 0.47%, 69.38% ± 0.65%, and 31.08% ± 0.41% in the three sequences groups respectively, compared to the blank group, the siCTGF-3 had the lowest level of CTGF expression (**Figure 4A**). The result of western blotting showed similar tendency (**Figure 4B**). Therefore, the siCTGF-3 appeared to have the optimum silencing efficiency.

Effect of Cs-siCTGF nanoparticles for inhibition of proteins' expression in a dose-dependent manner

To investigate the function of Cs-siCTGF nanoparticles, the fibroblasts were co-cultured with DMEM (blank), nanoparticles formed with scrambled RNA (Cs-siNC) or various concentrations of siCTGF (Cs-siCTGF-50 nM, Cs-siCTGF-100 nM and Cs-siCTGF-200 nM) respectively, fibrosis-related genes were detected by Western-blot and RT-PCR (**Figure 5**). The results of Western Blot demonstrated that chitosan/siCTGF nanoparticles could effectively inhibit the protein expression of CTGF, α-SMA and type I collagen in a dose-dependent manner, and there was no significant difference between blank and cells treated with Cs-siNC in all the proteins (**Figure 5A**). The mRNA expression level of CTGF were decreased to 76.03% ± 2.03%, 26.92% ± 3.67%, and 28.37% ± 2.23% in three treated groups compared with it in blank group (**Figure 5B**). In particular, the expression of CTGF in Cs-siCTGF-100 nM group and Cs-siCTGF-200 nM group was remarkably lower than it in the blank group and the Cs-siNC group. The mRNA expression level of α-SMA was decreased to 75.12 ± 1.14%, 55.14% ± 2.21%, and 59.76% ± 3.84% in three treated groups compared with it in blank group (**Figure 5C**). The mRNA level of collagen I was reduced

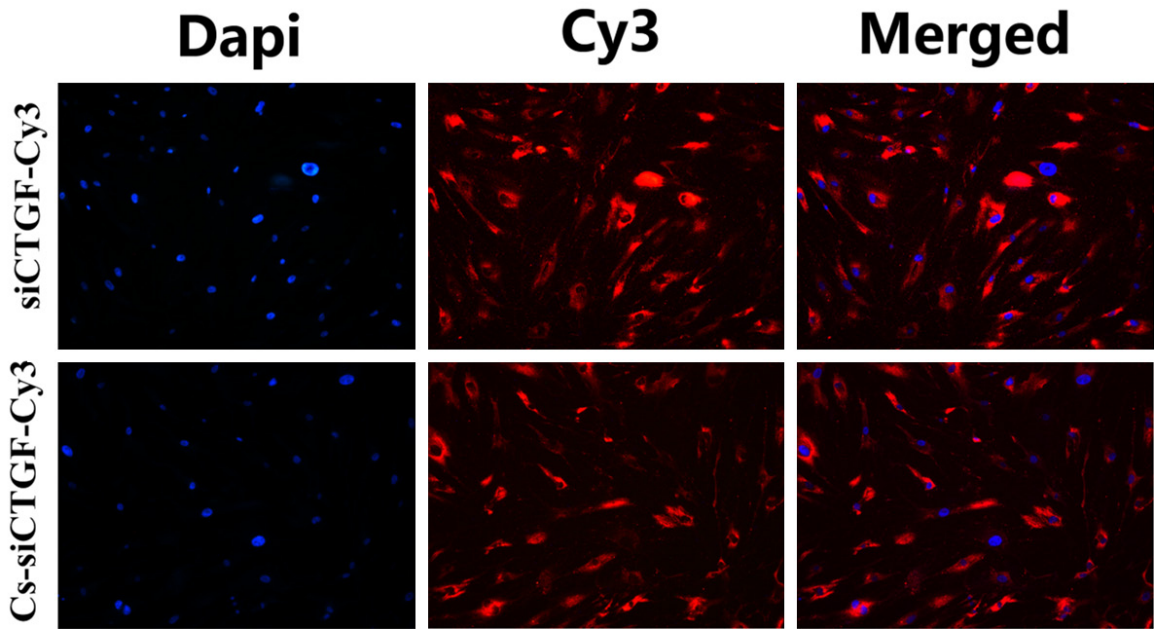

Figure 3. Fluorescence microscope detection of Cs-siCTGF nanoparticles on co-cultured fibroblasts. Fibroblasts were co-cultured with Cy3 dye labeled siCTGF (siCTGF-Cy3, top row) and Cs-siCTGF nanoparticles (Cs-siCTGF-Cy3, bottom row). After image merged, the Cy3-labeled siCTGF (red) appeared around the Dapi stained nuclear dots (blue) in the both Cs-siCTGF-Cy3 group and the Cs-siNC-Cy3 group. Scar bars: 200 μm.

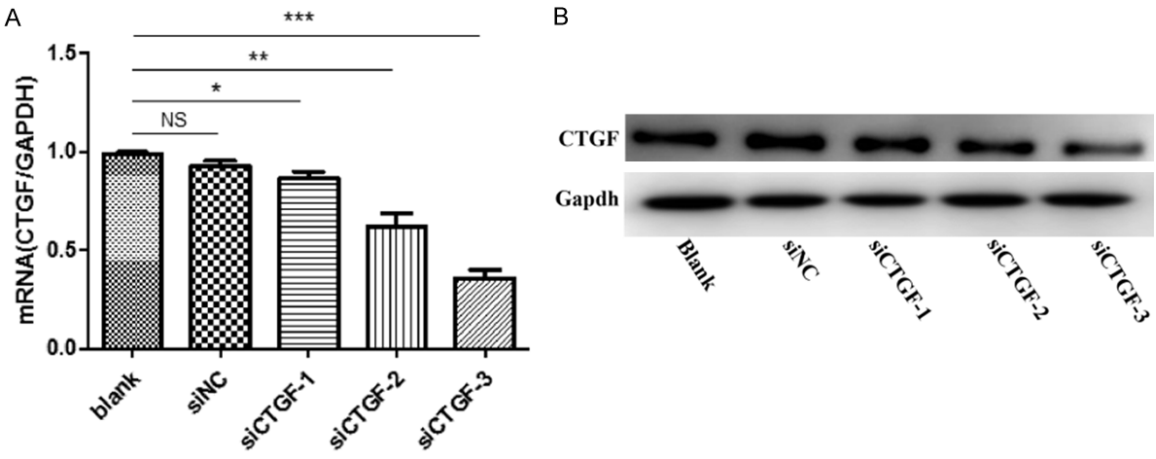

Figure 4. Selection of optimal siCTGF sequence. Three siCTGF sequences were designed and transferred into fibroblasts, the silencing efficiency of CTGF was detected at (A) mRNA level and (B) protein level. Data was shown as means ± SD, n=3; *P<0.05, **P<0.01, ***P<0.001. Scar bars: 100 μm.

to 73.12 ± 2.09%, 41.65% ± 3.77%, and 49.76% ± 2.61% in three treated groups compared with the blank group (**Figure 5D**). The above data showed both the Cs-siCTGF-100 nM group and Cs-siCTGF-200 nM group had the bigger inhibiting efficiency than other groups. However, there are no statistical differences between these two groups. These results demonstrated that Cs-siCTGF nanoparticles could effectively inhibit the expression of α-SMA and collagen I and CTGF in a dose-dependent manner.

Effect of Cs-siCTGF nanoparticles for elicitation of low toxicity to vital organs via local injection

To detect the accumulation and releasing time of Cs-siCTGF nanoparticles, Cy3 labeled con-

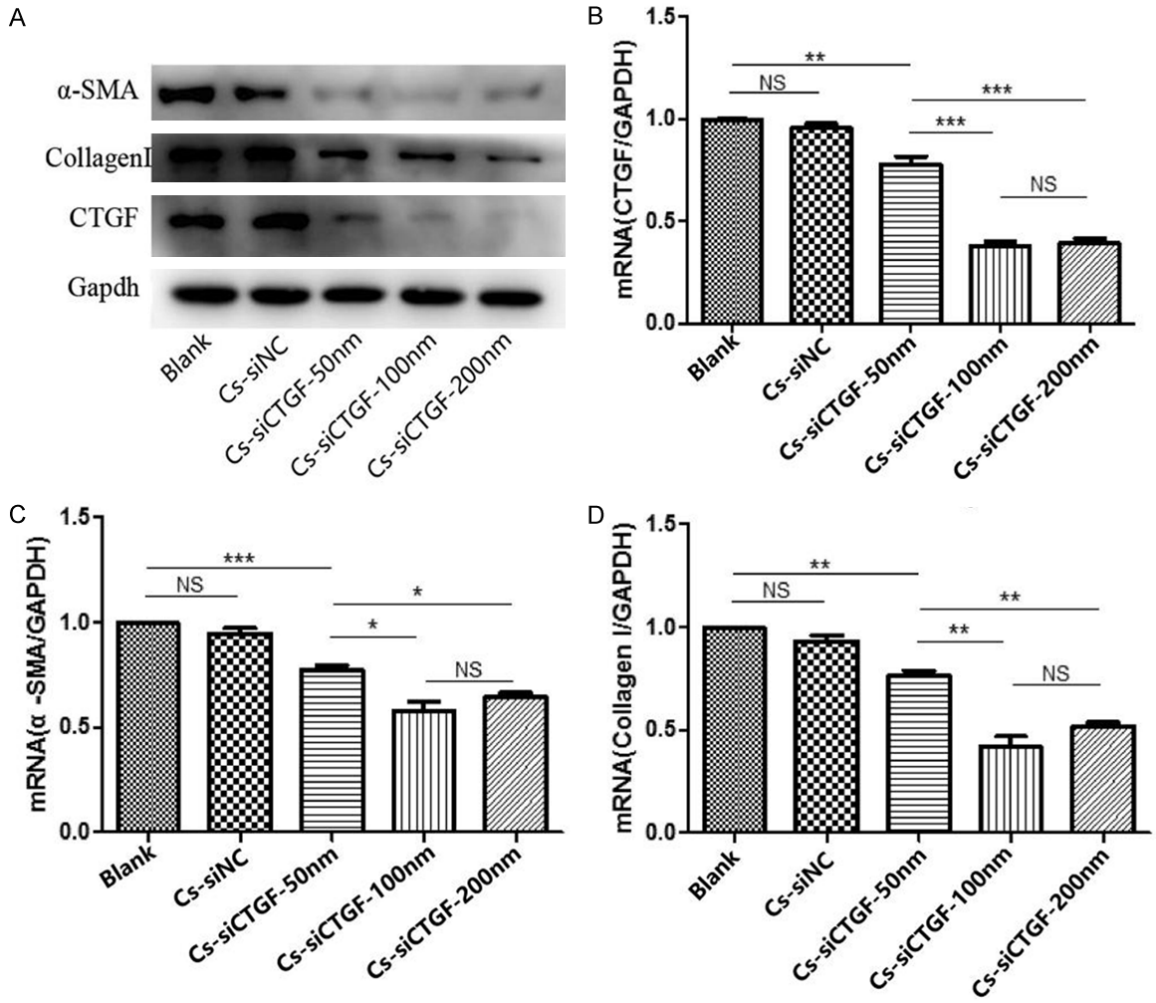

Figure 5. Effect of Cs-siCTGF nanoparticles on various proteins expression in fibroblasts. Fibroblasts were co-cultured with DMEM (blank), nanoparticles formed with scrambled RNA (Cs-siNC) or various concentrations of siCTGF (Cs-siCTGF-50 nM, Cs-siCTGF-100 nM and Cs-siCTGF-200 nM) respectively, fibrosis-related genes were detected. A. Representative mRNA level of α-SMA, Collagen I and CTGF in each treatment group, assayed by RT-PCR. B-D. Relative intensity of CTGF, α-SMA and Collagen I expressions normalized by GAPDH, assayed by western blotting. Data was shown as means ± SD, n=3; *P<0.05, **P<0.01, ***P<0.001. Scar bars: 100 μm.

trol siCTGF and Cs-siCTGF were injected intradermally from the edge of the wound in nude mice. At 1, 6, 24, 48, and 72 hours, the mice were anesthetized with 2.5% isoflurane, wound fluorescence position and intensity were detected by using an in vivo imaging system. In the control siCTGF-Cy3 group, the fluorescence signal (red color) appeared after 10 minutes and intensified at 6 hours, followed by gradually weakening and finally disappeared after 24 hours. In contrast, the fluorescence signal reached the peak at 24 hours in the Cs-siCTGF-Cy3 group, and the signal weakened and disappeared after 72 hours (**Figure 6A**, **6B**). In addition to the wound, other organs did not show evidence of fluorescence signal accumulation. This finding suggested that Cs-siRNA nanoparticles elicited low toxicity to vital organs via local injection.

Effect of Cs-siCTGF nanoparticles for attenuation of hypertrophic scar

For examining the function of siCTGF nanoparticles, the chitosan was loaded with the concentrations of siCTGF nanoparticles at 100 nM as treatment groups, DMEM (blank) and Cs-siNC nanoparticles were used as control groups. The wounds were made on the ventral ears of rabbits, granulation tissues were inject-

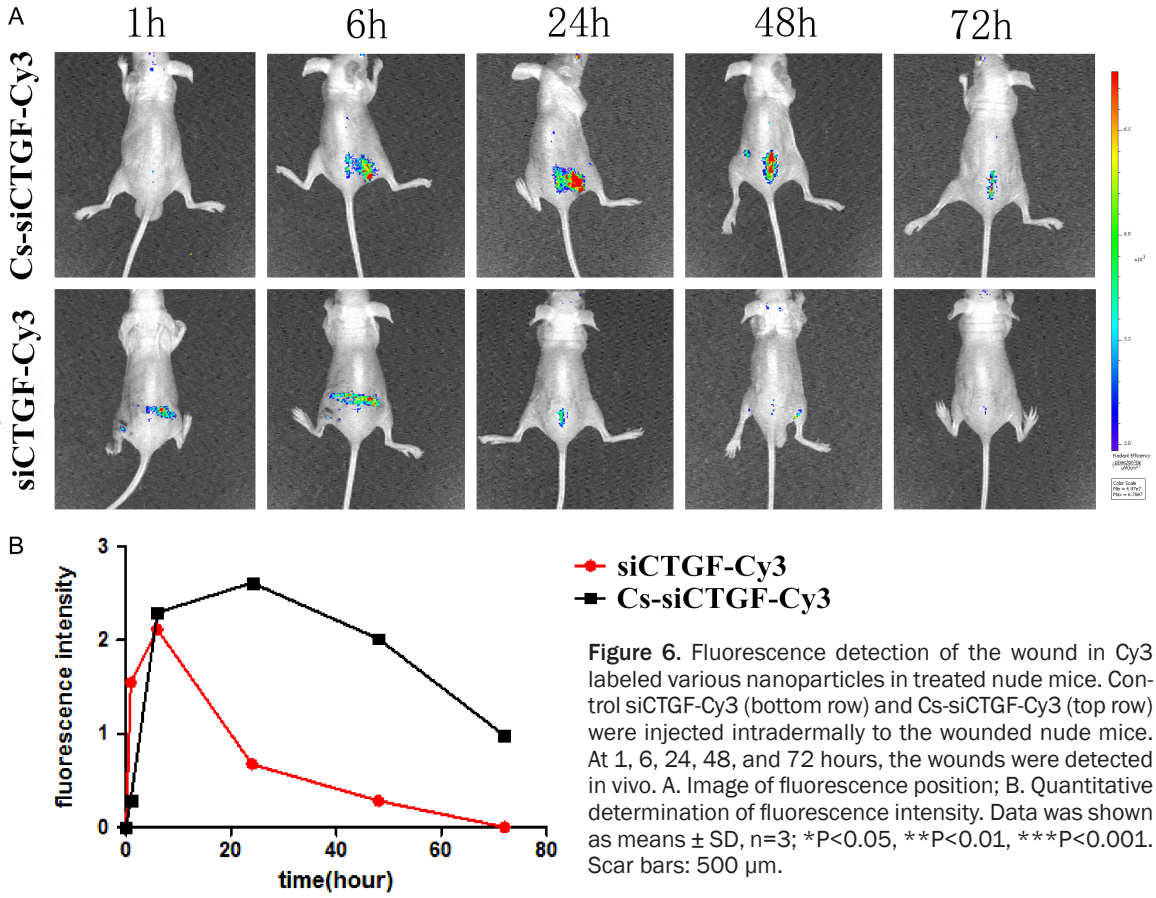

Figure 6. Fluorescence detection of the wound in Cy3 labeled various nanoparticles in treated nude mice. Control siCTGF-Cy3 (bottom row) and Cs-siCTGF-Cy3 (top row) were injected intradermally to the wounded nude mice. At 1, 6, 24, 48, and 72 hours, the wounds were detected in vivo. A. Image of fluorescence position; B. Quantitative determination of fluorescence intensity. Data was shown as means ± SD, n=3; *P<0.05, **P<0.01, ***P<0.001. Scar bars: 500 μm.

ed with either Cs-siNC or Cs-siCTGF for every three days from week 2 to improve transfection efficiency. General observation revealed that the scar thickness from the treatment group was improved at week 4 and week 8 (**Figure 7A**). The scar thickness on the rabbit's ear was measured by color Doppler ultrasound detectors, and was smaller in the Cs-siCTGF-100 nM group than it in the control groups (**Figure 7B** and **7C**). The Cs-siCTGF-100 nM group elicited the largest effect on scar reduction. The protein expression levels of α-SMA and CTGF were reduced in the treatment group by Immunohistochemistry staining (**Figure 8B**, **8C**). The result of Masson trichrome staining showed collagen deposition was improved in terms of size and irregular arrangement in the treatment group (**Figure 8A**).

Discussion

Hypertrophic scars are formed through scar tissue hyperplasia and are spread beyond the initial skin lesion area. Wound healing procedure is frequently accompanied by scar formation in adults. In the early stage, extremely activated fibroblasts promote wound healing and injury closure. However, in the late stage, excessive deposition of collagen and extracellular matrix (ECM) results in scar formation. The pathogenesis of hypertrophic scar involves many signaling pathways, among these, persistent activation of transforming growth factor-β (TGF-β)/Smad signaling plays an important role. However, direct targeting TGF-β or Smads genes may influence the overall effectiveness of such therapies. In contrast to TGF-β or Smads gene, down-regulation of CTGF can reduce scarring without influencing the overall effectiveness [12]. In light of these findings, CTGF is proposed as a profibrotic factor that plays an important role in the pathways of leading fibrosis, such as renal fibrosis and pulmonary fibrosis. Chitosan, derived from chitin, is orally non-toxic in animals and humans, and has been intensively investigated for drug and gene delivery [22, 23]. Glycol-chitosan, characterized by low molecular weight and water soluble derivation, were reported to selectively accumulate in the

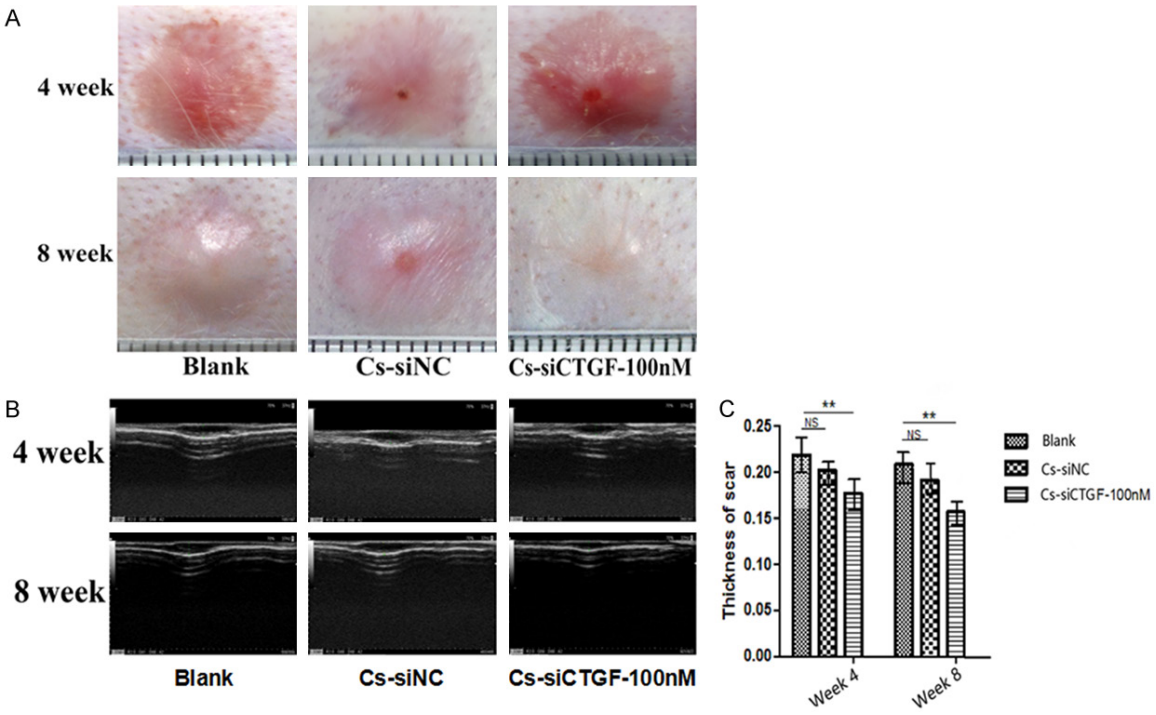

Figure 7. Effect of Cs-siCTGF nanoparticles in a wound generated rabbit model. The wounds were made on the ventral side of the ears of rabbits, granulation tissues were injected with either DMEM (blank) or Cs-siNC or Cs-siCTGF for every three days from week 2 to improve transfection efficiency. A. General observation of the scar thickness on the rabbit's ear. B. Thickness of the rabbit ear measured by color Doppler ultrasound detectors. C. Quantitative determination of thickness of scar. Data was shown as means ± SD, n=3; *P<0.05, **P<0.01, ***P<0.001. Scar bars: 500 μm.

mouse kidney renal tubules following i.v. injection, and thus could potentially be utilized to deliver drugs or other compounds to the kidneys [24].

In the present study we employed non-water-soluble chitosan polyplex nanoparticles as a vector/vehicle and successfully formed Chitosan/siCTGF (Cs-siCTGF) nanoparticles for therapy. For detecting the morphology of these nanoparticles, two methods were applied (**Figure 1A**, **1B**), compared the method of TEM, the hydration size of particles measured by dynamic light scattering could be bigger, because the particle size could be collapsed after negative staining of TEM. Cs-siCTGF nanoparticles sustained the release of siCTGF to approximately 72 hours and are not toxic to fibroblasts compared with siCTGF (**Figure 2A**, **2B**). In vitro, Cy3 dye labeled siCTGF (siCTGF-Cy3) and Cs-siCTGF nanoparticles (Cs-siCTGF-Cy3) were made and incubated with fibroblasts, the transfection and uptake rate of nanoparticles were observed, the merged image showed Cs-siCTFG-Cy3 could be entrapped in fibroblasts.

Meanwhile, the optimal sequence of siCTGF was designed and confirmed by detection of mRNA level (**Figure 4A**) and protein level (**Figure 4B**) of CTGF expression. Cs-siCTGF nanoparticles could reduce CTGF expression in fibroblasts successfully and affected the cell viability slightly. In our study, we utilized lentiviral transduction to perform RNA interference in fibroblasts, and found that down-regulation of CTGF expression could inhibit the proliferation of fibroblasts and formation of extracellular matrix (**Figure 5A-C**). It is similar with a previous study, which reported that CTGF is highly expressed in fibroblasts, and CTGF (-/-) fibroblasts are defective in cell migration and spreading [14, 19]. These results imply that CTGF has an important role in the fibrotic phenotype of fibroblasts.

Low treatment efficiency is usually caused by rapid clearance of naked siRNA *in vivo*. To achieve the silencing effect, it normally requires high dose of siRNA. In the other hand, the existing time of siRNA in serum should be shortened to impede its degradation effectively. Thus, the effective delivery of siRNA has become a great

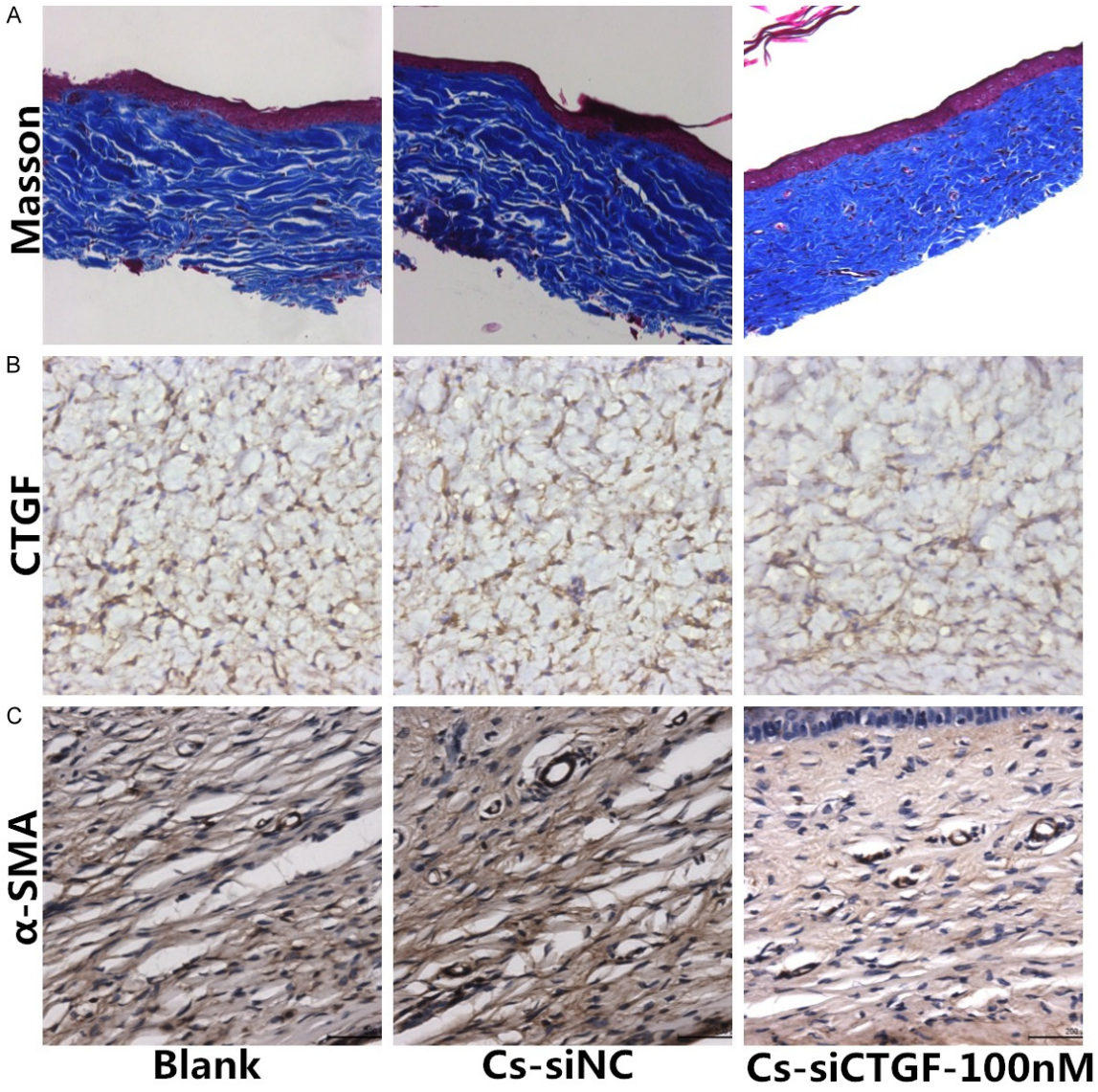

Figure 8. Effect of Cs-siCTGF nanoparticles on protein expression in wound generated rabbit model. The rabbits were given wound punches on the ventral side of the ears, granulation tissues were injected with either DMEM (blank) or Cs-siNC or Cs-siCTGF for every three days from week 2 to improve transfection efficiency. A. Representative protein deposition of Collagen by Masson trichrome staining. B. Representative protein expression of CTGF by immunohistochemistry staining. C. Representative protein expression of α-SMA by immunohistochemistry staining. Data was shown as means ± SD, n=3; *P<0.05, **P<0.01, ***P<0.001. Scar bars: 100 μm.

challenge. In this study, two methods were employed to overcome the problem. Compared with intravenous injection, localized dermal injection could directly reach the target organ (skin), reduce the risk of drug lost, and enhance the delivery efficiency of siRNA. It is similar with a previous study, which reported that direct joint injection of naked TNF-a siRNA inhibited joint inflammation [23]. Moreover, optical imaging systems are very well proven for tracking the fluorescence distribution and verifying whether Cs-siRNA nanoparticles can accumulate in the wound and sustained in a controlled release. Cs-siCTGF-Cy3 nanoparticles were observed in the accurate wound in nude mice (**Figure 6A**), the fluorescence signal reached the peak at 24 hours and the signal weakened and disappeared after 72 hours (**Figure 6B**), and other organs did not manifest fluorescence. This suggests that localized dermal injection could target intervention of local wounds and prevent side effects caused by

direct serum injection in vital organs. Meanwhile, to improve siRNA cellular entry without vector involvement, electroporation was confirmed to be a method for using. Studies have shown impressive therapeutic intervention in inflammation following i.v. administration of a cationic liposomal-based carrier [27].

Polymer nanoparticles have been widely used to improve the stability and pharmacokinetic properties of siRNA [27-29]. However, there are still a few problems in this study. First of all, this experiment only applied chitosan nanoparticles locally, without systemic delivery such as intravenous injection or intraperitoneal injection, which means that the delivery ability of nano-drug particles in the whole body to target organs or tissues could not be detected, and thus the ability to evade absorption and clearance of non-target tissues could not be detected. Secondly, it has been demonstrated that intravenous particles larger than 100 nm in diameter are likely to be trapped in the liver, spleen, lung and bone marrow by reticuloendothelial system (RES), leading to degradation of activated monocytes and macrophages. In our hands, although the particle size of the nanoparticles under the electron microscope was less than 100 nm, the average particle size detected in the solution was 190.4 ± 3.6 nm, so the possibility of degradation by macrophages may be greater. Finally, nanoparticles become unstable after storage or administration, which can lead to toxicity that is difficult to trace. Here, cytotoxicity was just detected in vitro, which was not continuously tracked in animal experiments. All the above problems need to be further supplemented or solved in future research.

In summary, this study demonstrates that down-regulation of CTGF expression by siCTGF reduced fibroblast proliferation and ECM production, and finally attenuated wound scarring in a rabbit hypertrophic scar model. Our study showed that Cs-siCTGF nanoparticles may be used as a promising therapy method in extenuate scar formation.

Acknowledgements

This work was funded by National Nature Science Foundation of China (8157080427).

Disclosure of conflict of interest

None.

Address correspondence to: Haibin Wu, Department of General Surgery, General Hospital of Central Theater Command, The People's Liberation Army, Wuhan 430070, Hubei, China. E-mail: whb152144@163.com; Yongjun Zheng, Burns Center of Changhai Hospital, The Second Military Medical University, Shanghai 200433, China. E-mail: smmuzhengyongjun@163.com

References

[1] Bock O, Schmid-Ott G, Malewski P and Mrowietz U. Quality of life of patients with keloid and hypertrophic scarring. Arch Dermatol Res 2006; 297: 433-8.

[2] Border WA and Noble NA. Transforming growth factor beta in tissue fibrosis. N Engl J Med 1994; 331: 1286-1292.

[3] Pena RA, Jerdan JA and Glaser BM. Effects of TGF-beta and TGF-beta neutralizing antibodies on fibroblast-induced collagen gel contraction: implications for proliferative vitreoretinopathy. Invest Ophthalmol Vis Sci 1994; 35: 2804-2808.

[4] O'Kane S and Ferguson MW. Transforming growth factor beta s and wound healing. Int J Biochem Cell Biol 1997; 29: 63-78.

[5] Cordeiro MF, Mead A, Ali RR, Alexander RA, Murray S, Chen C, York-Defalco C, Dean NM, Schultz GS and Khaw PT. Novel antisense oligonucleotides targeting TGF-beta inhibit in vivo scarring and improve surgical outcome. Gene Ther 2003; 10: 59-71.

[6] Penn JW, Grobbelaar AO and Rolfe KJ. The role of the TGF-beta family in wound healing, burns and scarring: a review. Int J Burns Trauma 2012; 2: 18-28.

[7] Lu L, Saulis AS, Liu WR, Roy NK, Chao JD, Ledbetter S and Mustoe TA. The temporal effects of anti-TGF-beta1, 2 and 3 monoclonal antibody on wound healing and hypertrophic scar formation. J Am Coll Surg 2005; 201: 391-7.

[8] Shah M, Foreman DM and Ferguson MW. Control of scarring in adult wounds by neutralising antibody to transforming growth factor beta. Lancet 1992; 339: 213-4.

[9] Wahl SM. Transforming growth factor beta (TGF-beta) in inflammation: a cause and a cure. J Clin Immunol 1992; 12: 61-74.

[10] Branton MH and Kopp JB. TGF-beta and fibrosis. Microbes Infect 1999; 1: 1349-1365.

[11] Sisco M, Kryger ZB, Jia SX, et al. Antisense oligonucleoides against transforming growth factor-beta delay wound healing in rabbit ear model. J Am Coll Surg 2005; 201: S60.

[12] Sisco M, Kryger ZB, O'Shaughnessy KD, Kim PS, Schultz GS, Ding XZ, Roy NK, Dean NM and Mustoe TA. Antisense inhibition of connective tissue growth factor (CTGF/CCN2) mRNA limits hypertrophic scarring without affecting wound

healing in vivo. Wound Repair Regen 2008; 16: 661-673.
[13] Gibson DJ, Pi L, Sriram S, Mao C, Petersen BE, Scott EW, Leask A and Schultz GS. Conditional knockout of CTGF affects corneal wound healing. Invest Ophthalmol Vis Sci 2014; 55: 2062-2070.
[14] Shome D, von Woedtke T, Riedel K and Masur K. The HIPPO transducer YAP and its targets CTGF and Cyr61 drive a paracrine signalling in cold atmospheric plasma-mediated wound healing. Oxid Med Cell Longev 2020; 2020: 4910280.
[15] Frazier K, Williams S, Kothapalli D, Klapper H and Grotendorst GR. Stimulation of fibroblast cell growth, matrix production, and granulation tissue formation by connective tissue growth factor. J Invest Dermatol 1996; 107: 404-11.
[16] Yokoi H, Sugawara A, Mukoyama M, Mori K, Makino H, Suganami T, Nagae T, Yahata K, Fujinaga Y, Tanaka I and Nakao K. Role of connective tissue growth factor in profibrotic action of transforming growth factor-beta: a potential target for preventing renal fibrosis. Am J Kidney Dis 2001; 38 Suppl 1: S134-8.
[17] Khoo YT, Ong CT, Mukhopadhyay A, Han HC, Do DV, Lim IJ and Phan TT. Upregulation of secretory connective tissue growth factor (CTGF) in keratinocyte-fibroblast coculture contributes to keloid pathogenesis. J Cell Physiol 2006; 208: 336-343.
[18] Igarashi A, Nashiro K, Kikuchi K, Sato S, Ihn H, Fujimoto M, Grotendorst GR and Takehara K. Connective tissue growth factor gene expression in tissue sections from localized scleroderma, keloid, and other fibrotic skin disorders. J Invest Dermatol 1996; 106: 729-33.
[19] Lipson KE, Wong C, Teng Y and Spong S. CTGF is a central mediator of tissue remodeling and fibrosis and its inhibition can reverse the process of fibrosis. Fibrogenesis Tissue Repair 2012; 5 Suppl 1: S24.
[20] Kanasty RL, Whitehead KA, Vegas AJ and Anderson DG. Action and reaction: the biological response to siRNA and its delivery vehicles. Mol Ther 2012; 20; 513-524.
[21] Bramsen JB, and Kjems J. Development of therapeutic-grade small interfering RNAs by chemical engineering. Front Genet 2012; 3: 154.
[22] Zhang X, Shan P, Jiang D, Noble PW, Abraham NG, Kappas A and Lee PJ. Small interfering RNA targeting heme oxygenase-1 enhances ischemia-reperfusion-induced lung apoptosis. J Biol Chem 2004; 279: 10677-84.
[23] Lu PY, Xie F and Woodle MC. In vivo application of RNA interference: from functional genomics to therapeutics. Adv Genet 2005; 54: 117-42.
[24] Dash M, Chiellini F, Ottenbrite RM and Chiellini E. Chitosan-A versatile semi-synthetic polymer in biomedical applications. Progress In Polymer Science 2011; 36: 981-1014.
[25] Ragelle H, Vandermeulen G and Preat V. Chitosan-based siRNA delivery system. J Control Release 2013; 172: 207-218.
[26] Howard KA, Rahbek UL, Liu X, Damgaard CK, Glud SZ, Andersen MØ, Hovgaard MB, Schmitz A, Nyengaard JR, Besenbacher F and Kjems J. RNA interference in vivo and vitro using a novel chitosan/siRNA nanoparticle system. Mol Ther 2006; 14; 476-484.
[27] Ma Z, Yang C, Song W, Wang Q, Kjems J and Gao S. Chitosan hydrogel as siRNA vector for prolonged gene silencing. J Nanobiotechnology 2014; 12: 23.
[28] Liu X, Howard KA, Dong M, Andersen MØ, Rahbek UL, Johnsen MG, Hansen OC, Besenbacher F and Kjems J. The influence of polymeric properties on chitosan/siRNA nanoparticle formulation and gene silencing. Biomaterials 2007; 28: 1280-1288.
[29] Katas H and Alpar HO. Development and characterisation of chitosan nanoparticles for siRNA delivery. J Control Release 2006; 115: 216-225.